



# The application research of benzyl methacrylate (BzMA) in acrylate latex pressure sensitive adhesives

Cheng Fang<sup>a,b,\*</sup>, Fuxiang Zhou<sup>b</sup>, Xiaolong Zhu<sup>b</sup>

<sup>a</sup> Jiangsu Co-Innovation Center of Efficient Processing and Utilization of Forest Resources, Nanjing Forestry University, Nanjing, 210037, People's Republic of China

<sup>b</sup> College of Chemical Engineering, Nanjing Forestry University, Nanjing, 210037, People's Republic of China

## ARTICLE INFO

### Keywords:

Cyclic methacrylate  
Benzyl methacrylate  
Emulsion polymerization  
Pressure sensitive adhesive

## ABSTRACT

The cyclic methacrylate monomer benzyl methacrylate (BzMA) was evaluated as an alternative to traditional methyl methacrylate (MMA) as a hard monomer in the application of an acrylate latex pressure sensitive adhesive (PSA). The influences of BzMA on the resultant latex and PSA properties were comprehensively investigated. Both FTIR and <sup>1</sup>H NMR analysis indicated that BzMA could be successfully introduced into the latex PSA copolymer through emulsion polymerization. TEM images illustrated that the synthesized latex particles are spherical and uniform. DSC and TGA results showed that the T<sub>g</sub> of the copolymer was elevated, while thermal stability was first increased and then decreased with the introduction of BzMA. Besides, it was also found that the water resistance of the latex PSA was improved by the presence of BzMA, which was confirmed by water contact angle measurements. Furthermore, as the BzMA content increased, the gel content slightly decreased, while sol molecular weight (M<sub>w</sub>, M<sub>n</sub>) of the polymer increased. Finally, with respect to the adhesive properties of the PSA, it was observed that loop tack decreased, while shear strength increased with the incorporation of BzMA. 180° peel strength initially increased and then decreased with the addition of BzMA from 0 to 30 wt%, with a maximum value at 5 wt%.

## 1. Introduction

Pressure sensitive adhesives (PSAs) are a special type of adhesive that can firmly adhere to a wide range of surfaces by the application of a light pressure (1–10 Pa) for a short contact time (1–5 s) [1,2], and that can be easily removed from the substrate without any residue [3]. They have been widely used including as packing and product labels, sticky notes, conducting coats, protective films, medical band-aids, etc [4]. The viscoelasticity, an optimal balance between elastic and dissipative properties, will significantly impact the final adhesive properties of a PSA that are usually characterized by tack, peel strength and shear strength [5]. Tack can be understood as the wettability of the PSA to the surface of a substrate, and peel strength is essential for the bond strength between PSA and an adherend, while shear strength shows the cohesive strength of the PSA. Commercial PSAs can be produced via hot-melt techniques, solution polymerization and emulsion polymerization; the latter, being considered more environmental friendly, was used to produce the PSAs in this study.

Major materials used in PSA formulations are natural rubber,

petroleum-based styrene-butadiene-styrene (SBS), polyisobutylene (PIB), nitrile rubber (NBR), polyurethanes and polyacrylates. In particular, polyacrylate emulsion PSAs are present in a large variety of applications in science, industries, and every-day life because of the low environment impact, balanced end-product properties, compatibility with additives and processability, competitive cost and oxidative ultraviolet resistance [6]. Other advantages of polyacrylate PSA dispersions are their high solids, their ease of application, and the fact that they may be formulated, in many instances, without the need for addition of tackifiers [7]. Among acrylate polymers used for making PSAs, long alkyl acrylates, such as poly(n-butyl acrylate, n-BA) [8] and poly(2-ethyl hexyl acrylate, 2-EHA) [9] are commonly used. However, because these kinds of acrylate PSAs comprise polymers that have high entanglement molecular weight (M<sub>c</sub>) [6] values, low glass transition temperature (T<sub>g</sub>) values, and medium to low molecular weights, this may present problems in PSA label converting and high temperature printing, and some types of cross-linking must be provided to yield shear holding power [10]. It is for such reasons that homopolymers are rarely used for pressure sensitive adhesive applications, although intraparticle

\* Corresponding author. Jiangsu Co-Innovation Center of Efficient Processing and Utilization of Forest Resources, Nanjing Forestry University, Nanjing, 210037, People's Republic of China.

E-mail address: [fangcheng533@163.com](mailto:fangcheng533@163.com) (C. Fang).

<https://doi.org/10.1016/j.ijadhadh.2021.102861>

cross-linking occurs as part of the chain transfer to the polymer during emulsion polymerization. The major challenge in the production of PSAs is to meet the conflicting properties that are required for application (tack, peel strength and shear resistance). To achieve this purpose, a PSA is usually a copolymer of an inherently tacky polymer (used to provide adhesion) with a higher  $T_g$  polymer used to increase cohesive strength. Copolymerization of acrylates with other monomers, such as methyl methacrylate (MMA), styrene (St) and vinyl acetate (VAc) is used to vary the chemical and physical properties of the PSA. For example, Xu et al. [11] prepared a series of acrylic water-borne PSAs with controlled composition and structure for the copolymerization of BA and AA with different MMA contents. They found that copolymerization of BA with MMA raised the glass transition temperature ( $T_g$ ) of the soft acrylic polymers, and had the effect of improving shear resistance, while the loop tack and peel adhesion were kept relatively high. Roberge, et al. [8] investigated the effect of particle size and composition on the performance of styrene/butyl acrylate miniemulsion-based PSAs. They found that an increase in styrene content resulted in higher peel strengths. However, at the largest particle sizes, the impact of adding more styrene to the recipe lowered the peel strength. Jovanovic, et al. [12] prepared butyl acrylate/vinyl acetate/acrylic acid (BA/VAc/AA) emulsion pressure sensitive adhesives through a semi-batch mode and investigated the influence of the individual monomer concentrations on final properties such as glass transition temperature ( $T_g$ ), peel strength, shear strength and tack. They found that the most significant factor affecting the final properties was the AA concentration, followed by the VAc concentration.

Benzyl methacrylate (BzMA) is widely used in nanoimprinting lithography, paint applications, inkjet inks, transparent adhesives, orthodontic adhesive compositions, and also as stationary phases in liquid chromatography [13]. However, as far as we know, no study to date has investigated the application of benzyl methacrylate (BzMA) as “hard” monomer in both emulsion polymerization and acrylate PSAs. The aim of the present work was to investigate systematically the effect of cyclic methacrylate monomer BzMA on the comprehensive properties of the acrylate latex PSA.

In this paper, a series of acrylate PSA latexes based on butyl acrylate (BA) and benzyl methacrylate (BzMA), together with acrylic acid (AA) and 2-hydroxyethyl acrylate (HEA) were synthesized via a monomer-starved seeded semi-continuous emulsion polymerization process. The chemical structure of the resultant polymer and the morphology of the latex particles were determined by FTIR, HNMR and TEM, respectively. Furthermore, the effects of BzMA on the conversion of monomer and particle size of the latex, as well as on the thermostability (DSC, TG), water contact angle, gel content, sol molecular weight ( $M_w$ ,  $M_n$ ) and adhesive properties of the polymer films were investigated. Finally, some results were compared with those obtained when using the conventional hard monomer MMA.

## 2. Experimental

### 2.1. Materials

Butyl acrylate (BA), acrylic acid (AA), 2-hydroxy ethyl acrylate (HEA), ammonium persulfate (APS) and sodium bicarbonate ( $\text{NaHCO}_3$ ) were purchased from Shanghai Lingfeng Chemical Co., Ltd. Benzyl methacrylate (BzMA) was purchased from Shanghai Aladdin Chemistry Co., Ltd. (Shanghai, China). Ammonium nonyl phenol ethoxylate sulfate surfactant (Rhodapex CO-436) was obtained from Shanghai Honesty Fine Chemical Co., Ltd. Ammonia (25 wt% in  $\text{H}_2\text{O}$ ) was obtained from Nanjing Chemical Reagent Co., Ltd. All reagents were used without further purification. Distilled deionized water ( $\text{DI-H}_2\text{O}$ ) was used throughout the study.

### 2.2. Emulsion polymerization

The synthetic route and formulation for the acrylate latex pressure sensitive adhesives with cyclic methacrylate BzMA are shown in Scheme 1 and Table 1, respectively. 25 g deionized water and 1.5 g CO-436 were added to a 500 mL four-neck roundbottom flask and were stirred rapidly to aid dissolution of the emulsifier. The monomer mixtures were then slowly added into the water-emulsifier mixture through a constant pressure funnel over a period of 20 min. After that, the pre-emulsion was stirred for a further 30 min.

Another 500 mL four-neck round-bottom flask with a reflux condenser, a thermometer and a mechanical stirrer was filled with 0.15 g of  $\text{NaHCO}_3$ , 6 g of pre-emulsion, 0.15 g of APS and 45 g of deionized water with a stirring rate of 270 rpm at 82–85 °C with stirring maintained for 30 min. Then both the remaining pre-emulsion and an APS aqueous solution (0.35 g of APS was dissolved in 24 g water) were added dropwise into the reacting mixture for 3.5 h. After the feed was completed, the reaction was allowed to proceed for an additional 1 h to increase monomer conversion. The latex was then cooled to room temperature and poured into a glass bottle for further characterization.

### 2.3. Characterization

#### 2.3.1. Conversion and coagulation

The degree of conversion was measured by gravimetric analysis. About 2 g of latex was weighed into an aluminum foil dish and dried at 105 °C to a constant weight. The solid content and the final conversion were calculated using equations (1) and (2), respectively:

$$\text{Solid content (wt\%)} = \frac{W_3 - W_1}{W_2 - W_1} \times 100 \quad (1)$$

where  $W_1$  is the weight of the aluminum foil dish,  $W_2$  and  $W_3$  are the weights of latex before and after drying, respectively.

$$\text{Conversion (wt\%)} = \frac{\text{Solid content (wt\%)} \times W_4}{W_5} \times 100 \quad (2)$$

where  $W_4$  is the total weight of all the materials added into the glass bottle before polymerization and  $W_5$  is the total weight of monomers.

The coagulum was collected from the bottle cap and 100-mesh filter screen and then dried at 105 °C to a constant weight. The coagulation was described as the weight of coagulum per total weight of monomer added.

#### 2.3.2. Particle size

Latex particle size and polydispersity index (PDI) were both measured using a dynamic light scattering (DLS) instrument (Malvern NanoS Zetasizer). The analyses were carried out at 25 °C, and every result was an average of three parallel measurements. The latex was diluted until the solid content was about 1%. The reported diameter is an intensity-weighted average particle size.

#### 2.3.3. FTIR analysis

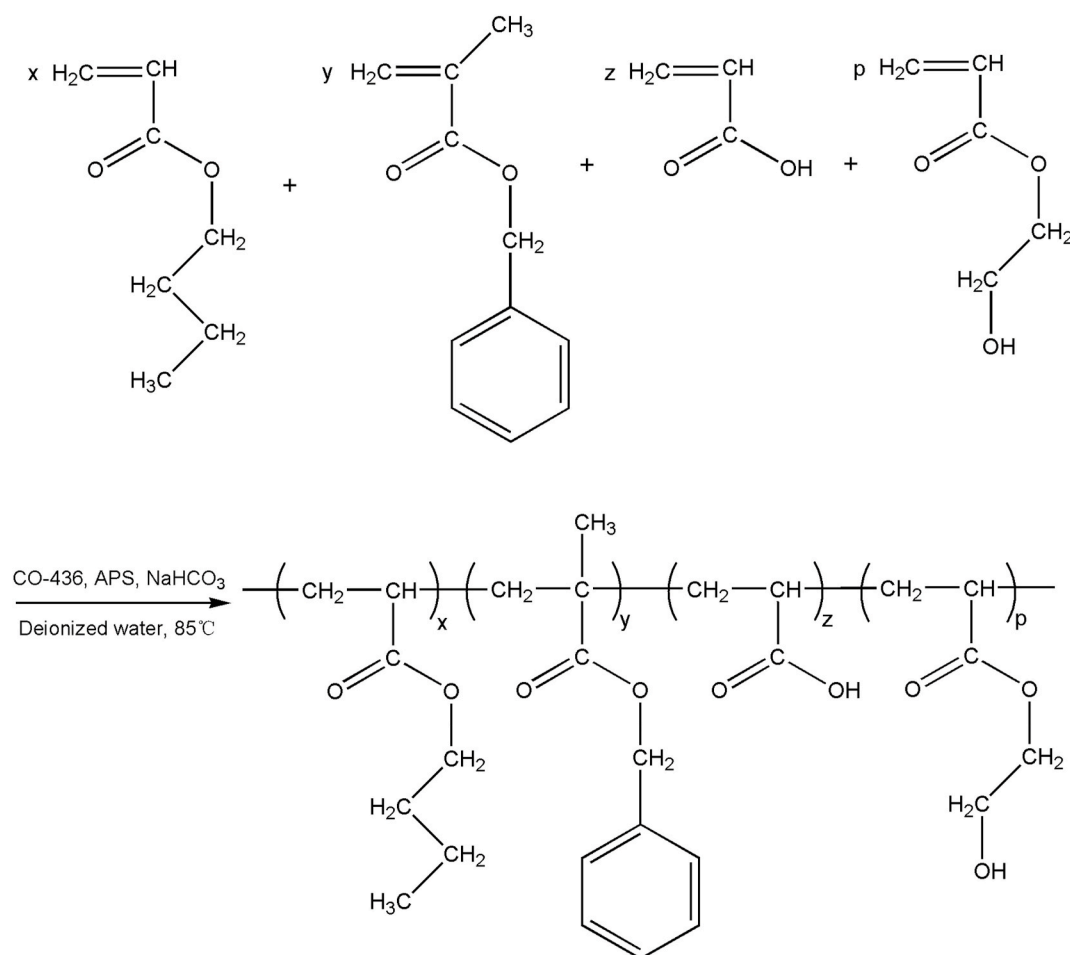
The latex was dried in a vacuum oven at 105 °C until it reached a constant weight. Fourier transform infrared (FTIR) spectra of the dried latex films were recorded with a Bruker VERTEX80 FTIR spectrometer (Germany) in the range 4000 to 400  $\text{cm}^{-1}$ .

#### 2.3.4. Nuclear magnetic resonance (NMR) analysis

$^1\text{H}$  NMR spectra were recorded on a Bruker AVANCE III 600 MHz NMR spectrometer at room temperature using  $\text{CDCl}_3$  as solvent with conventional tetramethylsilane (TMS) as internal standard.

#### 2.3.5. TEM analysis

The latex particle morphology was observed by transmission electron microscopy (TEM) (JEOL JEM-1400, Tokyo, Japan). The latex was



**Scheme 1.** Schematic diagram for the synthesis of acrylate latex PSAs with cyclic methacrylate BzMA.

**Table 1**

Compositions and amounts employed in the synthesis of the acrylate latex PSA.

| Compositions       |                    | Amount (g) |
|--------------------|--------------------|------------|
| Soft monomer       | BA                 | 67–97      |
| Hard monomer       | BzMA               | 0–30       |
| Functional monomer | AA                 | 1          |
|                    | HEA                | 2          |
| Emulsifier         | CO-436             | 1.5        |
| Initiator          | APS                | 0.5        |
| Buffer             | NaHCO <sub>3</sub> | 0.15       |
| Continuous phase   | Deionized water    | 94         |

diluted in deionized water to a 2 wt% solid content. Then the diluted latex was coated and dried on a 400-mesh carbon coated copper grid for assessment by TEM.

### 2.3.6. DSC analysis

Glass transition temperature ( $T_g$ ) of the latex film was measured by a differential scanning calorimeter (DSC, Model 214 Polyma, NETZSCH Instruments, Germany). 5–15 mg of dry polymer was weighed into a standard DSC hermetic alumina crucible. In order to eliminate thermal history, two scanning cycles of heating-cooling were performed for each sample at a heating rate of 10 °C/min within the temperature range of –70 to 100 °C under a nitrogen atmosphere. The second heating run was used to determine the  $T_g$ .

### 2.3.7. Thermal gravimetric analysis (TGA)

TGA was carried out to demonstrate the thermal stability of the latex

PSA polymers using Q500, TA Instruments, USA. The polymer films (around 5–10 mg) were heated from ambient temperature to 600 °C at a rate of 10 °C/min under a nitrogen atmosphere.

### 2.3.8. Gel content

The gel content of the acrylic PSA polymers was measured via the solvent-extraction method. Three samples (around 0.2 g) of the dried latex film were weighed and sealed in a PTFE coated membrane pouch. This was then placed in a Soxhlet extractor with tetrahydrofuran (THF), followed by refluxing for 24h. After the extraction process, the membrane pouch was removed and first dried in a fume hood for 3h and then in a vacuum oven at 70 °C until it reached a constant weight. The weight of the remaining dry gel was taken and the gel content was calculated using equation (3):

$$\text{Gel content} = \frac{\text{mass of the dry gel}}{\text{mass of the initial dry polymer}} \quad (3)$$

### 2.3.9. Molecular weight determination

The molecular weight, number average molecular weight ( $M_n$ ) and weight average molecular weight ( $M_w$ ) and molecular weight distribution ( $M_w/M_n$ ) of the soluble fraction of polymer were determined by using Agilent HPLC 1200 Infinity Series. The THF solution remaining from the gel content test was concentrated and analyzed for sol molecular weight. THF was used as the eluent and the flow rate was set at 1 mL/min. The internal temperature was set at 30 °C. Narrow polystyrene standards having a molecular weight range from 400 to  $1 \times 10^6$  were used for calibration.

### 2.3.10. Contact angle analysis

Water contact angles on the latex films were determined by a contact angle goniometer (Attension Theta, Biolin Scientific, Sweden) at 20 °C using the sessile drop method. The volume used was 4  $\mu$ L and the final data of each sample was an average of at least ten readings.

### 2.3.11. PSA testing

Loop tack, peel strength and shear holding power were measured according to the Pressure Sensitive Tape Council standards PSTC-6, PSTC-1, and PSTC-7, respectively [14]. Further details of these methods were given in our previous work [15].

## 3. Results and discussion

### 3.1. Characterization of latexes

Table 2 summarizes the latexes synthesized in this work as well as their main properties including coagulation, conversion, particle size and PDI values. The results indicated that all the experiments were completed successfully with final conversions exceeding 96% and negligible coagulums. The evolution of both instantaneous and overall conversion versus reaction time for the latex prepared with 20 wt% BzMA is presented in Fig. 1. Instantaneous conversion at a given time during the monomer addition period is defined as the percentage of the total monomer added up to that time converted to polymer. Overall conversion at a given time is the percentage of the total monomer added up to the end of the monomer addition period converted to polymer [16]. It can be seen from Fig. 1 that instantaneous conversion was higher than 80% during the polymerization time due to the starved monomer feeding conditions used, and hence the instantaneous copolymer composition was very close to that used in the feeding stream producing homogeneous copolymer chains along the reaction. Full conversion was reached after a postpolymerization process of 1 h.

Particle size distribution (PSD) is usually determined over a list of particle size ranges that covers nearly all sizes present in the sample. Particle dispersity index (PDI) is used to evaluate the dispersion of PSD [17]. The smaller the value of PDI, the better the homogeneity of the emulsion. Fig. 2 exhibits the particle size and particle size distribution curves for the acrylate PSA latexes with various contents of BzMA. It can be seen from Table 2 and Fig. 2 that the particle sizes range from 215 to 220 nm with a monomodal distribution of the particles ( $PDI < 0.05$ ) regardless of the amount of BzMA, which was mainly due to the excess use of emulsifier. Micelles are the primary nucleation loci in this system, and homogeneous nucleation was negligible here. In an effort to identify latex particle morphologies, TEM images were collected. Fig. 3 shows the TEM images of two representative latexes without and with 20 wt% BzMA, i.e. PSA-BzMA-0 and PSA-BzMA-20. It can be obviously seen that both the TEM micrographs presented regular spherical shape and good dispersion, which was consistent with the particle size and PSD results aforementioned.

### 3.2. FTIR analysis

The chemical structures of acrylate latex PSAs with various contents of BzMA were characterized by Fourier transform infrared (FTIR) spectroscopy. FTIR spectra of the three representative samples (i.e. PSA-

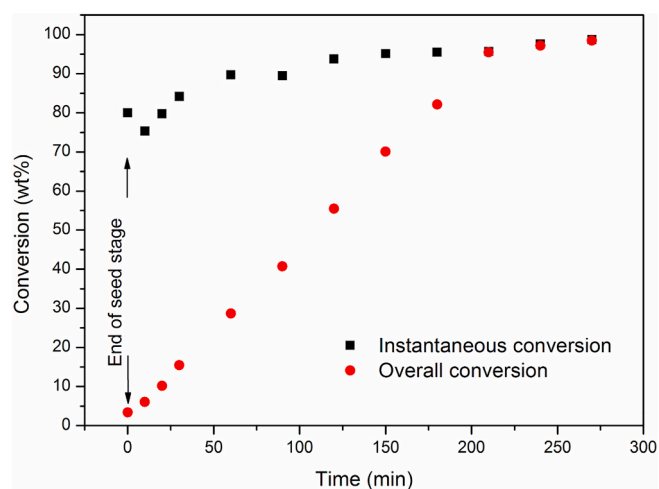


Fig. 1. Representative evolution of instantaneous and overall conversion during the synthesis of latex PSA-BzMA-20.

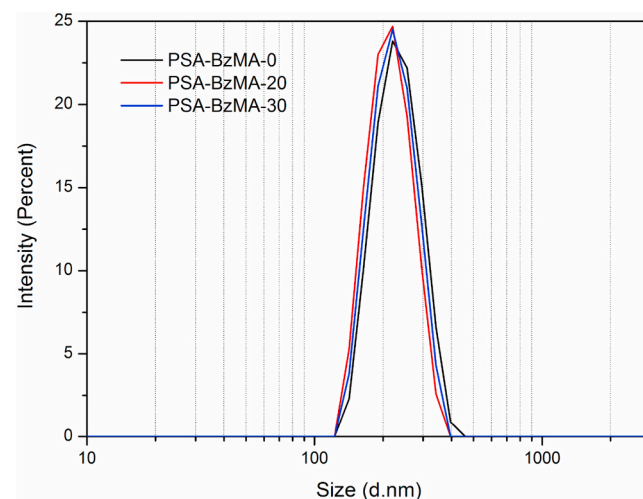


Fig. 2. Particle size and particle size distribution curves for the acrylate PSA latexes with different content of BzMA.

BzMA-0, PSA-BzMA-20, PSA-BzMA-30) are shown in Fig. 4. It can be clearly seen that all three spectra exhibit some similar peaks such as the characteristic stretching peaks of C–H ( $\text{CH}_2$ ) at 2958 and 2873  $\text{cm}^{-1}$ , stretching vibration of C=O at 1728  $\text{cm}^{-1}$ , and distortion vibration of  $\text{CH}_2$  at 1453 and 1378  $\text{cm}^{-1}$ , asymmetric and symmetric stretching vibration of C–O–C at 1240 and 1158  $\text{cm}^{-1}$ , as well as the absorption at 1063 and 941  $\text{cm}^{-1}$  resulting from characteristics of BA. On the other hand, after the introduction of BzMA into the recipe, both the spectra of PSA-BzMA-20 and PSA-BzMA-30 show the skeleton stretching vibration peak of a benzene ring at 1500  $\text{cm}^{-1}$ , and the monosubstituted peak of benzene at 738 and 697  $\text{cm}^{-1}$  [18,19]. And the more BzMA added, the stronger the peaks. Moreover, there is no adsorption peak at 1641  $\text{cm}^{-1}$  which is attributed to the characteristic of C=C bonds of the monomers.

Table 2

Summary and characteristics of the synthesized acrylate PSA latexes with different content of BzMA.

| PSA ID      | Formulation (wt% monomers) | Coagulation (%) | Conversion (%) | Particle size (nm) | PDI   |
|-------------|----------------------------|-----------------|----------------|--------------------|-------|
| PSA-BzMA-0  | BA/AA/HEA (97/1/2)         | 0.002           | 98.5           | 215                | 0.026 |
| PSA-BzMA-5  | BA/BzMA/AA/HEA (92/5/1/2)  | 0.015           | 97.9           | 218                | 0.033 |
| PSA-BzMA-10 | BA/BzMA/AA/HEA (87/10/1/2) | 0.042           | 97.2           | 220                | 0.013 |
| PSA-BzMA-20 | BA/BzMA/AA/HEA (77/20/1/2) | 0.065           | 96.8           | 216                | 0.002 |
| PSA-BzMA-30 | BA/BzMA/AA/HEA (67/30/1/2) | 0.089           | 96.5           | 220                | 0.015 |



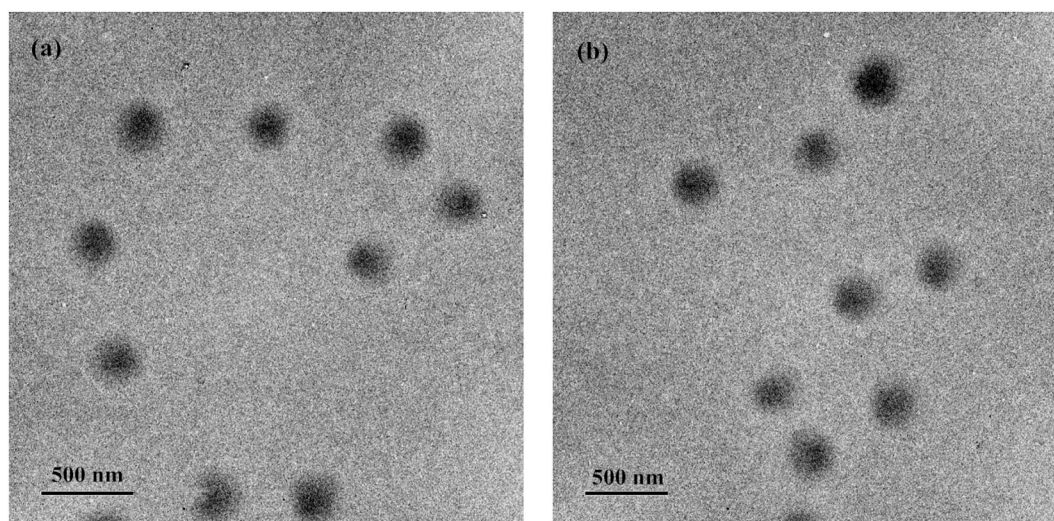


Fig. 3. TEM images of the acrylate PSA latex particles without (a) and with 20 wt% (b) BzMA.

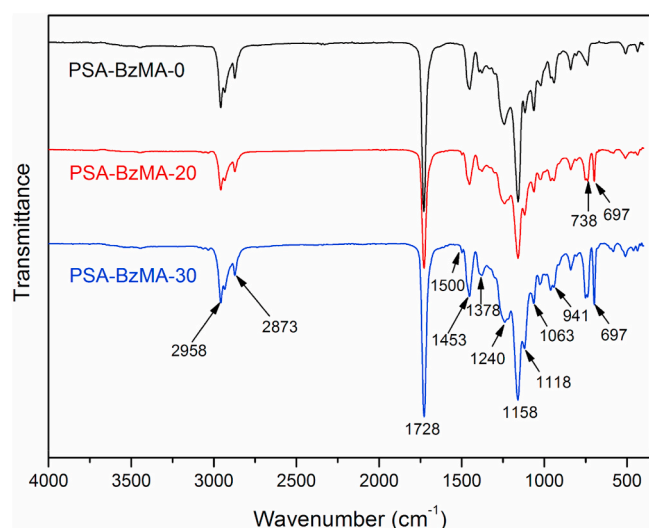


Fig. 4. FTIR spectra of acrylate latex PSAs with various contents of BzMA.

### 3.3. $^1\text{H}$ NMR analysis

Nuclear magnetic resonance technology was further adopted to characterize the chemical structure of the acrylate latex PSA copolymer containing 30 wt% BzMA, and the  $^1\text{H}$  NMR spectrum is presented in Fig. 5. It can be seen that the peak at 7.34 ppm reveals phenyl ring protons and the signal at 4.95 ppm assigned to methylene which is adjacent to oxygen in the BzMA unit. Both FTIR and  $^1\text{H}$  NMR results confirmed that cyclic methacrylate monomer BzMA has been successfully introduced into the acrylate latex PSA copolymer through emulsion polymerization.

### 3.4. DSC analysis

Glass transition temperature ( $T_g$ ) is one of the most important factors affecting PSA performance. A higher  $T_g$  commonly shows the higher rigidity of the PSA chains, which might manifest itself in better elasticity and cohesive behaviour. On the contrary, PSAs with lower  $T_g$  will demonstrate better fluidity or deformability, which makes for better tack but might cause cohesive failure. Fig. 6 displays the DSC curves of the acrylate latex PSAs with different BzMA contents. It is evident that all latex PSAs show similar curves with only one characteristic

endothermic peak indicating the presence of a homogeneous polymer. As shown in Fig. 6, the  $T_g$  of the PSA containing BzMA increased from  $-41.4^\circ\text{C}$  to  $-17.6^\circ\text{C}$  with the concentration of BzMA increasing from 0 to 30 wt%. The reason for this is that the  $T_g$  of BzMA homopolymer is reported to be around  $54^\circ\text{C}$  [20], which is much higher than the  $T_g$  of PBA ( $-54^\circ\text{C}$  [13]), resulting in the  $T_g$  of the copolymer increasing greatly with the incorporation of BzMA. On the other hand, it can be seen from Fig. 6 that the  $T_g$ s of the PSAs prepared with BzMA were a little lower than those prepared with MMA [21]. This phenomenon is consistent with the relationship between the  $T_g$  of BzMA homopolymer ( $54^\circ\text{C}$ ) and its MMA counterpart ( $105^\circ\text{C}$  [22]).

### 3.5. TG analysis

The thermal stability of the obtained acrylate latex PSAs with different amounts of BzMA were evaluated using thermogravimetric analysis (TGA). The TGA curves of the acrylate latex PSAs are shown in Fig. 7 with some results summarized in Table 3. It is evident that the thermal degradation behaviors of all the latex films occurred by a single-step degradation mechanism.

Ozlem [23] proposed that for P(n-BA), thermal degradation proceeds through simultaneous and subsequent processes,  $\gamma$ -hydrogen transfer from main chain to carbonyl group, transesterification reactions causing loss of butanol, and generation of six-membered products stabilized by cyclization reactions being among the major decomposition routes. It can be observed from Fig. 7 and Table 3 that thermal stability of the acrylate latex PSAs was improved as the amount of BzMA increased from 0 to 10 wt%. This may be ascribed to the incorporation of another monomer that will interfere with the chain reaction of decomposition. The degradation mechanism may be the same as for homopolymer of MMA and St, but the activation energy has changed [24]. However, when the amount of BzMA exceeds 10 wt%, the thermal stability of the acrylate latex PSA decreases. That is, as the size of the alkyl group increases the thermal stability decreases, probably due to an improvement in its interaction with the main chain which favors the chain scission to occur at a lower temperature [25].

### 3.6. Contact angle analysis

The hydrophobicity of the material is significantly affected by its surface chemical composition and is usually estimated by the contact angle (CA) [26]. Moreover, the higher CA value means stronger hydrophobicity and also better water resistance of the films [27]. The CA values of the acrylate latex PSA films with different amounts of BzMA

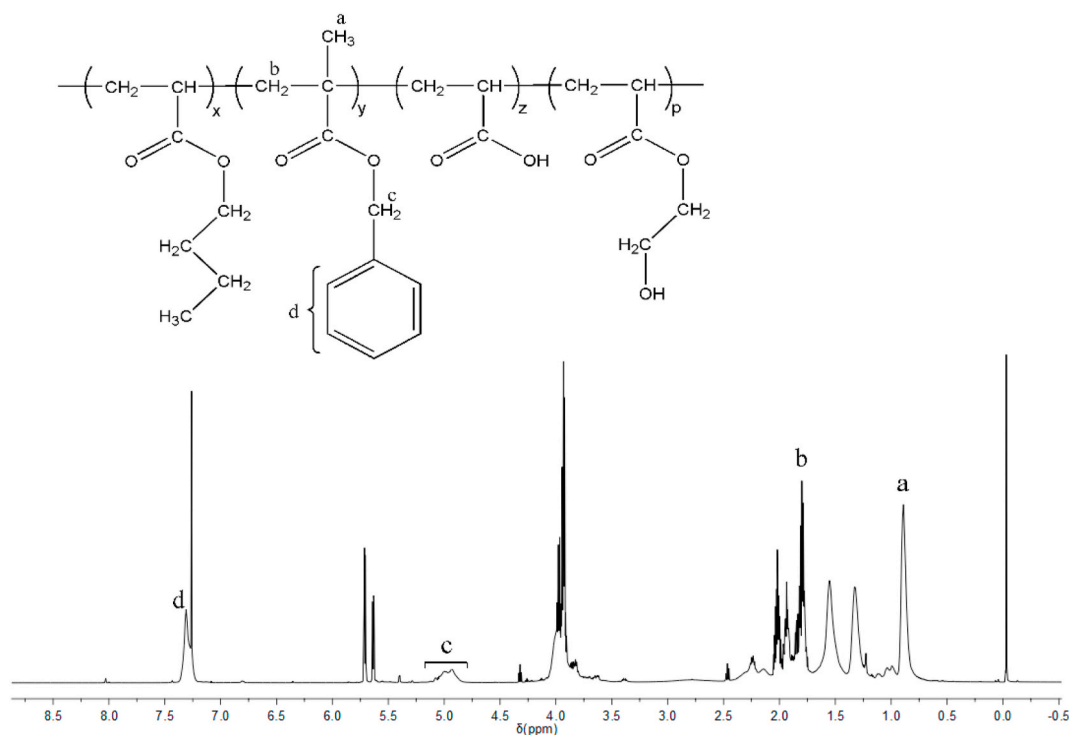


Fig. 5.  $^1\text{H}$  NMR spectrum of the acrylate latex PSA containing 30 wt% BzMA in  $\text{CDCl}_3$ .

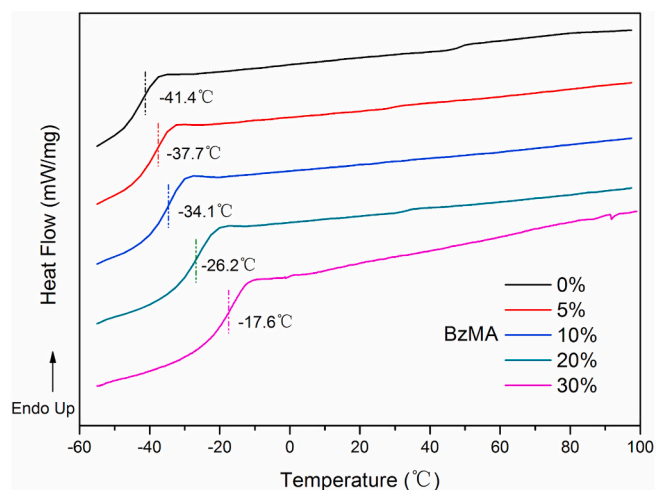


Fig. 6. DSC curves of acrylate latex PSAs with different content of BzMA.

and MMA are shown in Fig. 8. It can be seen from Fig. 8 that as the amount of BzMA increased from 0 to 30 wt%, the CA value of the film increased from  $96^\circ$  to  $122^\circ$ , indicating that the incorporation of cyclic methacrylate BzMA into the latex PSA copolymers increases the water contact angle and thus the water resistance of the latex films. Obviously, the enhanced hydrophobicity is mainly related to the presence of benzene ring structure of BzMA. And the water solubility of BzMA (0.4 g/L at  $25^\circ\text{C}$  [28]) was reported smaller than that of BA (2 g/L at  $25^\circ\text{C}$  [29]). On the other hand, it can be seen from Fig. 8 that the introduction of MMA would decrease the water contact angle and thus weaken the water resistance of the PSA films. This is mainly because the water solubility of MMA (11 g/L at  $25^\circ\text{C}$  [30]) is much higher than that of BA [29].

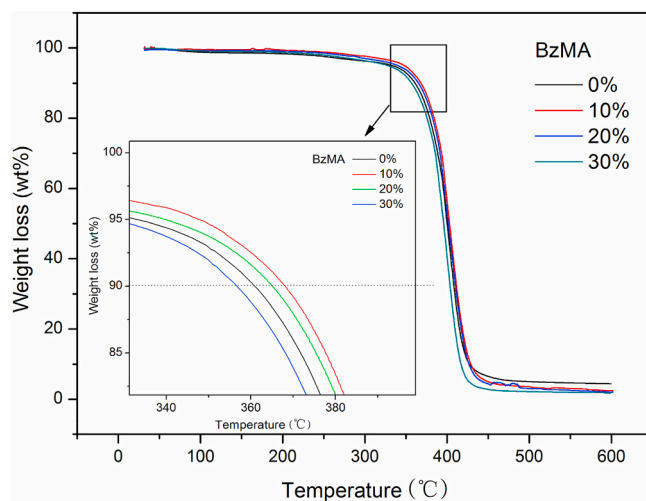


Fig. 7. TG curves of the acrylate latex PSAs with different amounts of BzMA.

Table 3

TGA and DTG results of the acrylate latex PSAs.

| Latex ID    | $T_5^a$<br>( $^\circ\text{C}$ ) | $T_{15}^a$<br>( $^\circ\text{C}$ ) | $T_{50}^a$<br>( $^\circ\text{C}$ ) | $T_{\max}^b$<br>( $^\circ\text{C}$ ) | Char residue<br>(%) |
|-------------|---------------------------------|------------------------------------|------------------------------------|--------------------------------------|---------------------|
| PSA-BzMA-0  | 333                             | 371                                | 399                                | 403                                  | 4.44                |
| PSA-BzMA-10 | 341                             | 371                                | 398                                | 401                                  | 3.59                |
| PSA-MMA-10  | 348                             | 387                                | 413                                | 416                                  | 3.86                |
| PSA-BzMA-20 | 338                             | 369                                | 396                                | 400                                  | 2.88                |
| PSA-BzMA-30 | 327                             | 368                                | 395                                | 399                                  | 1.83                |

<sup>a</sup>  $T_5$ ,  $T_{15}$  and  $T_{50}$  are referred to the temperature with 5%, 15% and 50% weight loss, respectively.

<sup>b</sup> The temperature at maximum decomposition rate ( $T_{\max}$ ).

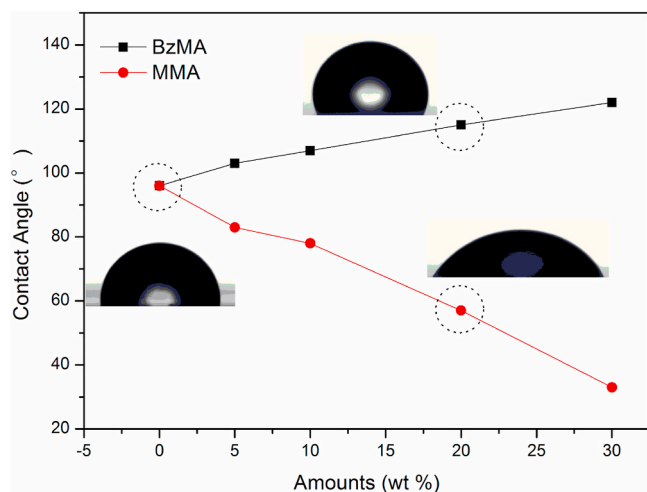


Fig. 8. CA of the acrylate latex PSA films with different amounts of BzMA and MMA.

### 3.7. Gel content and sol molecular weight analysis

Gel content is an important parameter, which contributes to the adhesion performance of PSAs and has been shown to be strongly influenced by the hard monomers. As we know, when a BA-rich monomer mixture is polymerized in the absence of cross-linker, gel is formed by either intermolecular or intramolecular chain transfer to polymer via backbiting, plus termination by combination [31]. The gel content and sol molecular weight of the acrylate latex PSAs with different amounts of BzMA are shown in Table 4. It can be clearly seen that the gel content was reduced from 60.5% to 44.6% as the amount of BzMA increased from 0 to 30 wt%. This can be attributed to the significantly lower activity for hydrogen abstraction of the methacrylic units in the polymer chain [32] due to the lack of labile hydrogens (see Fig. 9) in the molecular structure after BzMA participation into the polymerization as comonomer. This in turn leads to a reduction in chain transfer to polymer and branching, thus decreasing the gel content of the polymer. In the meantime, it can be seen from Table 4 that the sol molecular weight ( $M_w$ ,  $M_n$ ) of the acrylate latex PSAs was increased and MWD became wider with BzMA concentration which was mainly due to the transformation of the gel polymer to sol parts.

### 3.8. Adhesive properties

The adhesive properties were evaluated using tack, peel strength and shear strength measurements [33]. The results of experimental measurements of the adhesive properties of the acrylate latex PSAs with different amounts of BzMA are presented in Figs. 10 and 11. It can be clearly seen from Fig. 10 that loop tack gradually decreased from 10.08 N to 7.92 N, while shear strength greatly increased from 158 min to 3076 min with the amount of BzMA increased from 0 to 30 wt% which was mainly attributed to the elevated  $T_g$  as shown in Fig. 6. On the other hand, it is well known that peel strength generally decreases with an increase in the  $T_g$  of the PSA [34], but at the same time it can be

Table 4

Gel content and sol molecular weight of the acrylate latex PSAs with different amounts of BzMA.

| PSA ID      | Gel content (wt%) | $M_w$ (kg/mol) | $M_n$ (kg/mol) | $M_w/M_n$ |
|-------------|-------------------|----------------|----------------|-----------|
| PSA-BzMA-0  | 60.5 ± 1.291      | 178            | 57             | 3.21      |
| PSA-BzMA-5  | 57.2 ± 1.325      | 199            | 57             | 3.49      |
| PSA-BzMA-10 | 54.6 ± 0.876      | 221            | 58             | 3.81      |
| PSA-BzMA-20 | 50.1 ± 0.942      | 267            | 60             | 4.45      |
| PSA-BzMA-30 | 44.6 ± 0.503      | 315            | 68             | 4.63      |

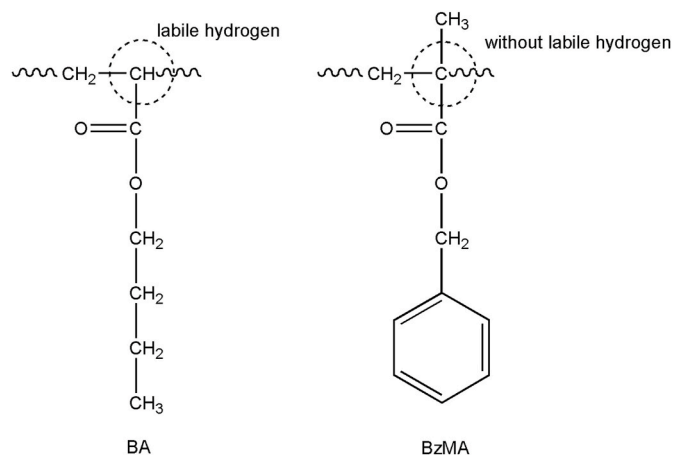


Fig. 9. Structure diagram of BA and BzMA after copolymerization.

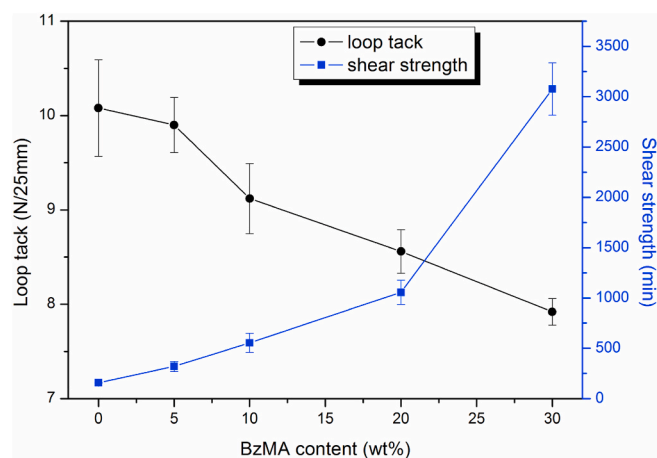


Fig. 10. Loop tack and shear strength of the acrylate latex PSAs with different content of BzMA.

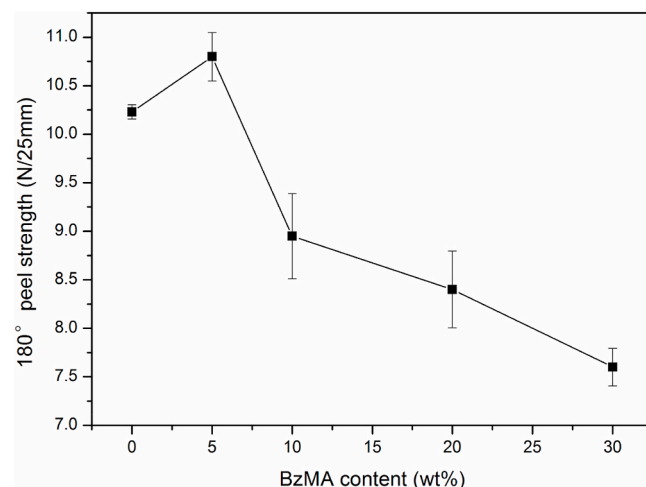


Fig. 11. 180° peel strength of the acrylate latex PSAs with different content of BzMA.

increased by lowering the gel content of the PSA [9]. The effect of BzMA on the peel strength of the acrylate latex PSA in this study may be a combination of these two aspects. It can be observed in Fig. 11 that peel strength initially increased and then decreased with the addition of



BzMA from 0 to 30 wt%, with a maximum value at 5 wt%. The reason for the increase in peel strength when BzMA amount was varied from 0 to 5 wt% was that the gel content of the PSA was decreased (see Table 4). As for the decrease in peel strength of the PSA when BzMA amount was increased from 5 wt% to 30 wt%, the reason might be that the positive effect on the peel strength, caused by lowering the gel content, could no longer counterbalance the negative effect caused by the increase in  $T_g$ .

#### 4. Conclusions

In this paper, a series of acrylate emulsion pressure sensitive adhesives (PSA), consisting of butyl acrylate (BA), benzyl methacrylate (BzMA), acrylic acid (AA) and 2-hydroxyethyl acrylate (HEA), were successfully prepared via a monomer-starved seeded semi-continuous emulsion polymerization process. Based on FTIR and  $^1\text{H}$  NMR results, it is confirmed that BzMA was successfully introduced into the latex PSA copolymer. TEM images illustrated that the synthesized latex particles are spherical and uniform. DSC and TGA results showed that  $T_g$  of the copolymer was elevated, while thermal stability was first increased and then decreased with introduction of BzMA. Besides, the contact angle of the acrylate latex PSA film was increased with increase in the amount of BzMA. Furthermore, as BzMA amount increased, gel content slightly decreased, while sol molecular weight ( $M_w$ ,  $M_n$ ) of the polymer increased. The shear strength was improved with BzMA content while at the sacrifice of loop tack. 180° peel strength of the PSA was initially increased and then decreased with the BzMA content.

#### Acknowledgment

We express our great gratitude to Nanjing Forestry University College Student Innovation Training Program Project (2020NFUS-PITP0076), Scientific Research of High-level (Highly educated) Talents of Nanjing Forestry University (GXL2018038) and Priority Academic Program Development of Jiangsu Higher Education Institutions (PAPD) for their financial support. The test supports from the teachers of Advanced Analysis & Testing Center of Nanjing Forestry University are also greatly appreciated.

#### References

- [1] Benedek I, Feldstein MM. Handbook of pressure-sensitive adhesives and products fundamentals of pressure sensitivity. Boca Raton (FL), London (MN), New York (NY): CRC, Taylor & Francis; 2009.
- [2] Ebnesajjad S, Landrock AH. Adhesives technology handbook. William Andrew; 2014.
- [3] Callies X, Herscher O, Fonteneau C, et al. Combined effect of chain extension and supramolecular interactions on rheological and adhesive properties of acrylic pressure-sensitive adhesives. ACS Appl Mater Interfaces 2016;8:33307–15.
- [4] Yu Q, Yang W, Wang Q, Dong W, Du M, Ma P. Functionalization of cellulose nanocrystals with gamma-MPS and its effect on the adhesive behavior of acrylic pressure sensitive adhesives. Carbohydr Polym 2019;217:168–77.
- [5] Mojtaba TS, Diba G. Rheological and adhesion properties of acrylic pressure sensitive adhesives. J Appl Polym Sci 2011;120(1):411–8.
- [6] Tobing SD, Klein A. Molecular parameters and their relation to the adhesive performance of acrylic pressure-sensitive adhesives. J Appl Polym Sci 2001;79: 2230–44.
- [7] Gower MD, Shanks RA. The effect of varied monomer composition on adhesive performance and peeling master curves for acrylic pressure-sensitive adhesives. J Appl Polym Sci 2004;93:2909–17.
- [8] Roberge S, Dubé MA. The effect of particle size and composition on the performance of styrene/butyl acrylate miniemulsion-based PSAs. Polymer 2006; 47:799–807.
- [9] Kajtna J, Likozar B, Golob J, Krajnc M. The influence of the polymerization on properties of an ethylacrylate/2-ethyl hexylacrylate pressure-sensitive adhesive suspension. Int J Adhesion Adhes 2008;28:382–90.
- [10] Wang T, Lei C, Dalton AB, Creton C, Lin Y, Fernando KAS, Sun Y, Manea M, Asua JM, Keddie JL. Waterborne, nanocomposite pressure-sensitive adhesives with high tack energy, optical transparency, and electrical conductivity. Adv Mater 2006;18:2730–4.
- [11] Xu H, Wang N, Qu T, Yang J, Yao Y, Qu X, Lovell PA. Effect of the MMA content on the emulsion polymerization process and adhesive properties of poly(BA-co-MMA-co-AA) latexes. J Appl Polym Sci 2012;123:1068–78.
- [12] Jovanovic R, McKenna TF, Dubé MA. Empirical modeling of butyl acrylate vinyl acetate acrylic acid emulsion based pressure sensitive adhesives. Macromol Mater Eng 2004;289:467–74.
- [13] Lapsa K, Marcinkowska A, Rachocki A, Andrzejewska E, Goc JT. Spectroscopic and photopolymerization studies of benzyl methacrylate poly(benzyl methacrylate) two-component system. J Polym Sci Pol Phys 2010;48:1336–48.
- [14] Pressure Sensitive Tape Council. Test methods for pressure sensitive adhesive tapes. Northbrook, Illinois: Pressure Sensitive Tape Council; 2004.
- [15] Fang C, Jing Y, Zong Y, Lin Z. Effect of N,N-dimethylacrylamide (DMA) on the comprehensive properties of acrylic latex pressure sensitive adhesives. Int J Adhesion Adhes 2016;71:105–11.
- [16] Treviño ME, Dubé MA. Synthesis of self-crosslinkable water-borne pressure sensitive adhesives. Macromol React Eng 2013;7:484–92.
- [17] Sun YF, Zhao XF, Liu RP, Chen G, Zhou XD. Synthesis and characterization of fluorinated polyacrylate as water and oil repellent and soil release finishing agent for polyester fabric. Prog Org Coating 2018;123:306–13.
- [18] Xie M, Chen F, Liu J, Yang T, Yin S, Lin H, Xue Y, Han S. Synthesis and evaluation of benzyl methacrylate-methacrylate copolymers as pour point depressant in diesel fuel. Fuel 2019;255:115880.
- [19] Worzakowska M. Starch-g-poly(benzyl methacrylate) copolymers Characterization and thermal properties. J Therm Anal Calorim 2016;124:1309–18.
- [20] Roka N, Pitsikalis M. Statistical copolymers of N-vinylpyrrolidone and benzyl methacrylate via RAFT: monomer reactivity ratios thermal properties and kinetics of thermal decomposition. J Macromol Sci 2018;55(3):222–30.
- [21] Fang C, Zhu X, Cao Y, Xu X, Wang S, Dong X. Toward replacement of methyl methacrylate by sustainable bio-based isobornyl methacrylate in latex pressure sensitive adhesive. Int J Adhesion Adhes 2020;100:102623.
- [22] Lovell PA, El-Aasser MS. Emulsion polymerization and emulsion polymers. New York: John Wiley and Sons; 1997.
- [23] Ozlem S, Hacaloglu J. Thermal degradation of poly(n-butyl methacrylate), poly (nbutyl acrylate) and poly(t-butyl acrylate). J Anal Appl Pyrol 2013;104:161–9.
- [24] Zhang L, Liu G, Ji R, Yao Y, Qu X, Yang L, Gao J. Thermal analysis, glass transition temperature and rheological behaviour of emulsion copolymers of methyl methacrylate with styrene. Polym Int 2003;52:74–80.
- [25] Isusi M, Rodríguez M, Garay T, Vilas JL, León LM. Thermal properties of copolymers of N-vinylcarbazole with acrylic and methacrylic monomers. J Macromol Sci B 2006;41(2):241–53.
- [26] Gong Y, Shao T, Chen X, Cao S, Chen L. Silicone acrylate dispersion based on semi-continuous seed emulsion polymerization using polymerizable emulsifiers. Chem Pap 2020;74:2875–82.
- [27] Wu J, Wang C, Mu C, Lin W. A waterborne polyurethane coating functionalized by isobornyl with enhanced antibacterial adhesion and hydrophobic property. Eur Polym J 2018;108:498–506.
- [28] Cockram AA, Neal TJ, Derry MJ, Mykhaylyk OO, Williams NSJ, Murray MW, Emmett SN, Armes SP. Effect of monomer solubility on the evolution of copolymer morphology during polymerization-induced self-assembly in aqueous solution. Macromolecules 2017;50:796–802.
- [29] Arellano J, Flores J, Zuluaga F, Mendizabal E, Katime I. Effect of monomer water solubility on cationic microemulsion polymerization of three components (water, surfactant, and monomer). J Polym Sci Pol Chem 2011;49:3014–9.
- [30] Kaczun J, Funke W. Molecular design of reactive microgels. Die Angewandte Makromolekulare Chemie 1996;240:99–112.
- [31] Plessis C, Arzamendi G, Leiza JR, Schoonbrood HAS, Charmot D, Asua JM. Seeded semibatch emulsion polymerization of n-butyl acrylate. Kinetics and structural properties. Macromolecules 2000;33:5041–7.
- [32] Asua M, Degrandi-contraires E, Lopez A, Reyes Y, Creton C. High-shear-strength waterborne polyurethane/acrylic soft adhesives. Macromol Mater Eng 2013;298: 612–23.
- [33] Jovanović R, Dubé MA. Emulsion-based pressure-sensitive adhesives: a review. J Macromol Sci Polym Rev 2004;44:1–51.
- [34] Guo J, Severton SJ. Optimizing the monomer composition of acrylic water-based pressure-sensitive adhesives to minimize their impact on recycling operations. Ind Eng Chem Res 2007;46:2753–9.